Supporting Information 2 for the manuscript:
"Metal-Assisted and Microwave-Accelerated Evaporative Crystallization" by Pinard and Aslan.
Corresponding author e-mail: kadir.aslan@morgan.edu

Characterization of glycine crystals with powder X-ray diffraction (XRD). XRD data for glycine crystals placed in a capillary tube with thin walls (0.02 mm) were collected using an in-house X-ray generator (MicroMax 7, Rigaku/MSC, The Woodlands, TX) and a Raxis4^{++} image plate detector (Rigaku/MSC), which is housed at the Core Facilities of the Department of Pharmaceutical Sciences, University of Maryland School of Pharmacy. The distance between the detector and samples were kept constant at 75 mm. The radiation source was CuKα (wavelength: 0.54 nm). The 2-D XRD data was collected at $0° \leq \delta \leq 120°$ at values of $0° \leq 2\theta \leq 40°$.

The collected 2-D XRD data (in .OSC format) was converted to ".IMG" and ".PS" formats using ADXV software (http://www.scripps.edu/~arvai/adxv.html). 1-D Intensity vs. 2θ plots was obtained by fitting the ".IMG" files using FIT2D software (http://www.esrf.eu/computing/scientific/FIT2D/). The polymorph reflections (e.g. $\alpha(020)$ were determined by comparing the peak locations in the 2θ plots for the experimental (Figure S10-S12).and simulated XRD patterns (Figure S13).

Simulated XRD patterns for α-, β-, and γ-glycine were generated using Mercury (Cambridge Crystallographic Data Center, Cambridge, United Kingdom, version 2.3). The crystallographic parameters for glycine crystals (CIF files) were obtained from published papers. [1,2]

Although optical microscopy and SEM images provide semi-quantitative information about the type of the glycine polymorphs due to the observable large size of crystals, the XRD data is more definitive. Figure S10 shows the 2-D XRD data for crystals grown from a glycine solution (3.2 M, pH =6) on glass at room temperature and using microwave heating. The XRD data also corroborate that the observation made by microscopy that a mixture of α- and γ-glycine was grown on glass at room temperature and using microwave heating. The intensity of reflections from glycine crystals grown on glass at room temperature was larger than those grown using microwave heating, which indicates the larger number of crystals grown at room temperature, as again evidenced by SEM and optical microscope images. It is important to note that identical glycine solution was used. In Figure S10A, the intensity of peaks for $\alpha(011)$, $\alpha(110)$ and $\alpha(020)$ are the largest indicating that glycine crystals are grown preferentially along these faces. Figure S14 (Top-Left) shows the depiction of the morphology for α-glycine crystals grown on glass at room temperature with these observed crystal faces. It is also interesting to note that bi-pyrmidal α-glycine crystals are formed through hydrogen bonding that is strongest in the bc- plane (011) and ab- plane (110). In addition, XRD data (Figure S10) shows that γ-glycine was preferentially grown along the (101) face on glass slides.

Figure S11 shows that only α-glycine was grown on SIFs at room temperature and using microwave heating. It is important to remind that the crystallization on SIFs occurred much faster than on glass slides due to the presence of multiple silver nanoparticles within close proximity serving as nucleation/growth sites. This can be explained as in the following: once the initial glycine molecules are adsorbed onto silver nanoparticles through their amine groups, the subsequent glycine molecules are selectively assembled onto the first glycine molecules through the carboxylic acid groups (that is, Silver---[NH$_2$—COOH]----[NH$_2$—COOH]---- [NH$_2$—COOH]----]. The assembling of glycine molecules occur faster under microwave heating due to the temperature gradient between the solution and the silver nanoparticles.[3] In this regard, it is also thought that microwave heating lowers the activation energy for the hydrogen bonding between glycine molecules, effectively speeding up the crystallization process. On the other hand, the assembly of glycine molecules at room temperature takes up to 20 minutes due to the absence of the driving force (temperature gradient) for the rapid transfer of glycine molecules from the solution to the nucleation sites on the surface of the silver nanoparticles.
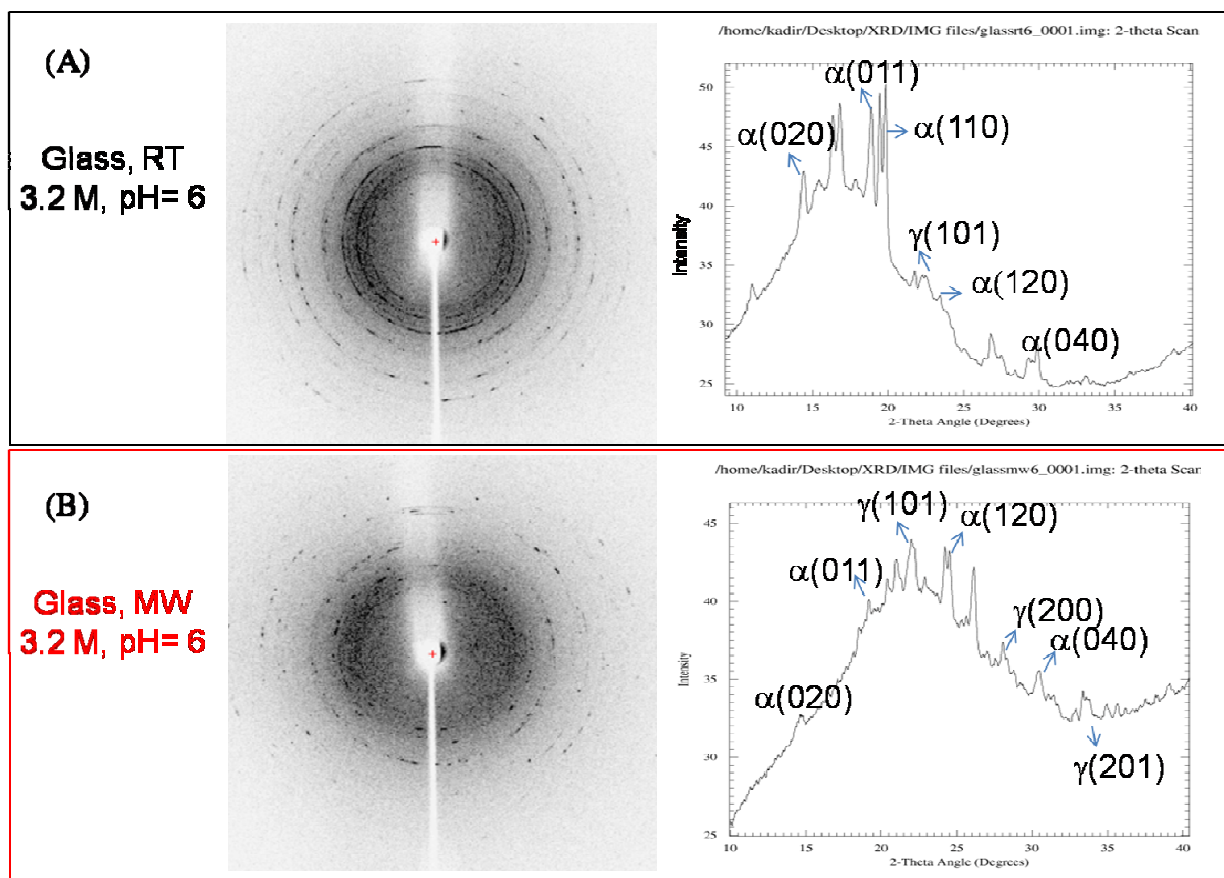
Figure S10. Experimental 2-D (Left) and 1-D (Right) Powder X-Ray Diffraction patterns of glycine crystals grown from glycine solutions 3.2 M pH= 6 on glass (A) at room temperature (RT) and (B) using microwave heating (MW). The Greek letters on the 1-D plots indicate the type of glycine polymorph that the peak belongs, which was determined by comparing the simulated XRD pattern for all three polymorphs given in Figure S13. The Miller indices correspoding to the peaks are also shown. The bell-shape in the 1-D plot is due to the background signal as also observed in the previus publications by others.[4,5]

It is also interesting to note a notable difference between the α-glycine crystals grown on glass at room temperature and on SIFs using microwave heating. As shown in the XRD data (Figures S10A and S11B), for α-glycine crystals grown on glass a strong peak at ~20° corresponding to the (110) face and a weak peak at ~24° corresponding to the (120) face appears. Conversely, for α-glycine crystals grown on SIFs, the intensity for the peak corresponding to the (120) face is stronger and the peak at ~20° corresponding to the (110) face is not present. The side-by-side comparison of the predicted α-glycine crystals morphology for crystals grown on glass at room temperature and on SIFs using microwave heating is shown in Figure S14-Top. Optical microscope and SEM images (Figure S2 and S8) show that the growth of α-glycine crystals on glass occurred preferentially in the z-direction (into the solution; x-y is glass surface), where glycine molecules were assembled onto smaller number of nucleation sites on glass. In comparison, the growth of α-glycine crystals on SIFs preferentially occurred in the x-y direction (on the surface), resulting in longer crystals due to the availability of large number of nucleation/growth sites (i.e. silver nanoparticles).
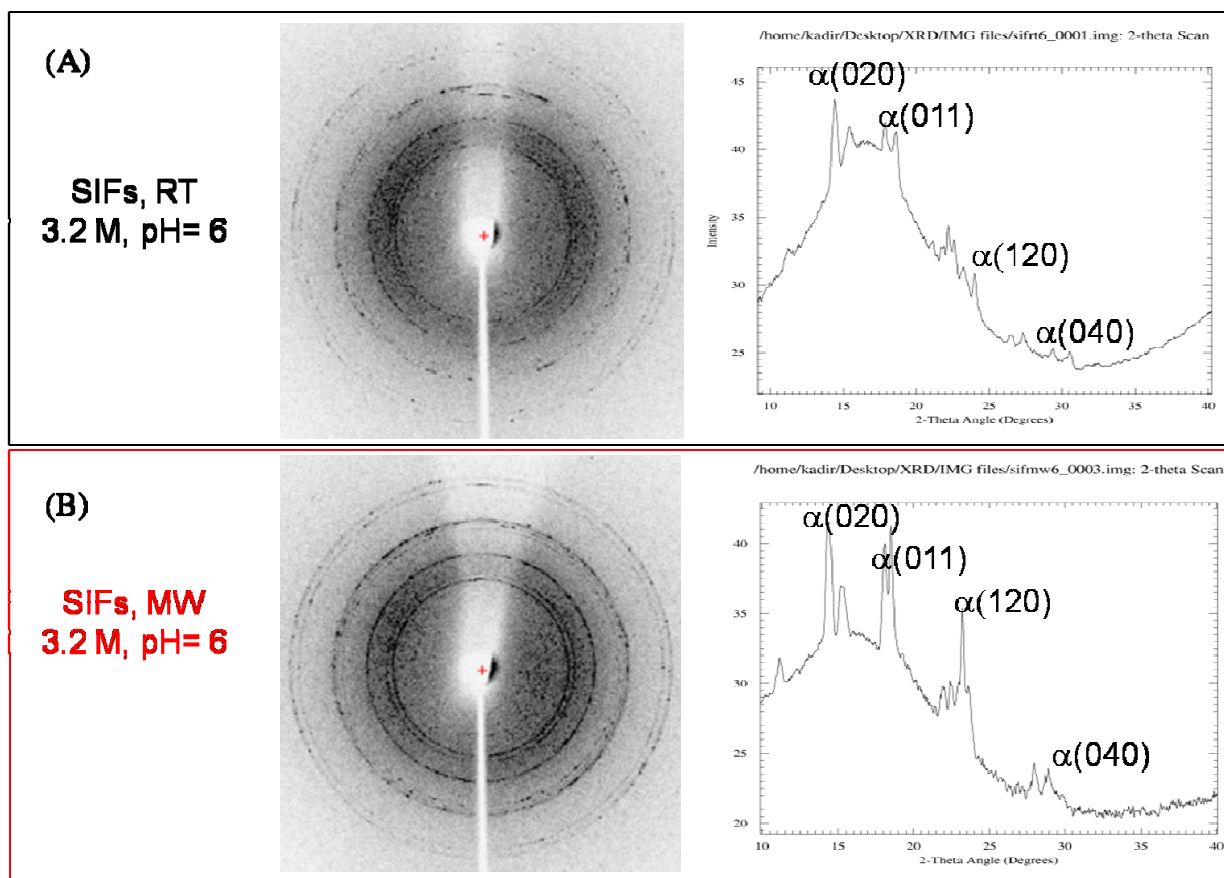
Figure S11. Experimental 2-D (Left) and 1-D (Right) X-Ray Diffraction patterns of glycine crystals grown from glycine solutions 3.2 M pH= 6 on SIFs (A) at room temperature (RT) and (B) using microwave heating (MW). The Greek letters on the 1-D plots indicate the type of glycine polymorph that the peak belongs, which was determined by comparing the simulated XRD patterns for all three polymorphs given in Figure S13. The Miller indices correspoding to the peaks are also shown.

β-glycine crystals were also observed from some of the samples. Figure S12 shows the XRD results for crystals grown from a 1.6M, pH=9 glycine solution on glass at room temperature and from a 3.2M, pH=9 glycine solution on SIFs using microwave heating. Once again, the reflections from α-glycine and γ-glycine were dominant, and in both the samples β(001) and β(110) reflections were present. The presence of β(001) and β(110) reflections indicate that β-glycine crystals were grown as plates.

It is known that the heating of glycine solutions to higher temperatures results in the transformation of γ-form into α- and β-forms.[6] This is due to the fact that α- and γ-glycine are enantiotropically related and such transformation occurs at high temperatures.[6] The existence of the high energy β-form can be explained by the high supersaturation process resulted by rapid evaporation of water.[6] The presence of γ-glycine on the surface after the crystallization process ended indicates the incomplete tranformation of γ-glycine into into α- and β-forms. Figure S14-Middle and S14-Bottom show the predicted β- and γ-glycine crystals morphology for crystals grown on glass at room temperature and on SIFs using microwave heating.
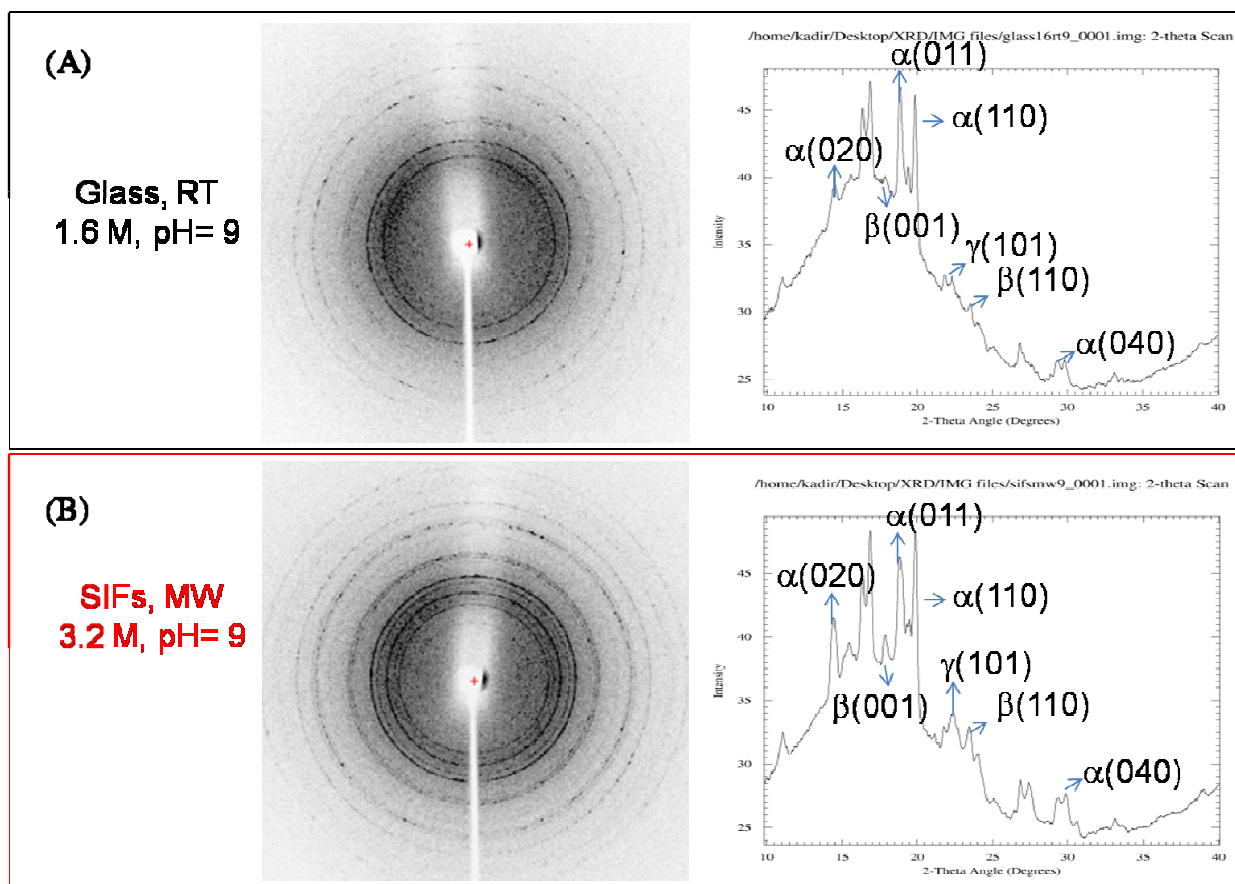
Figure S12. Experimental 2-D (Left) and 1-D (Right) patterns of glycine crystals grown from glycine solutions (A) 1.6 M pH= 9 on glass at room temperature (RT) and (B) 3.2 M pH= 9 on SIFs using microwave heating (MW). The Greek letters on the 1-D plots indicate the type of glycine polymorph that the peak belongs, which was determined by comparing the simulated XRD pattern for all three polymorphs given in Figure S13. The Miller indices correspoding to the peaks are also shown.
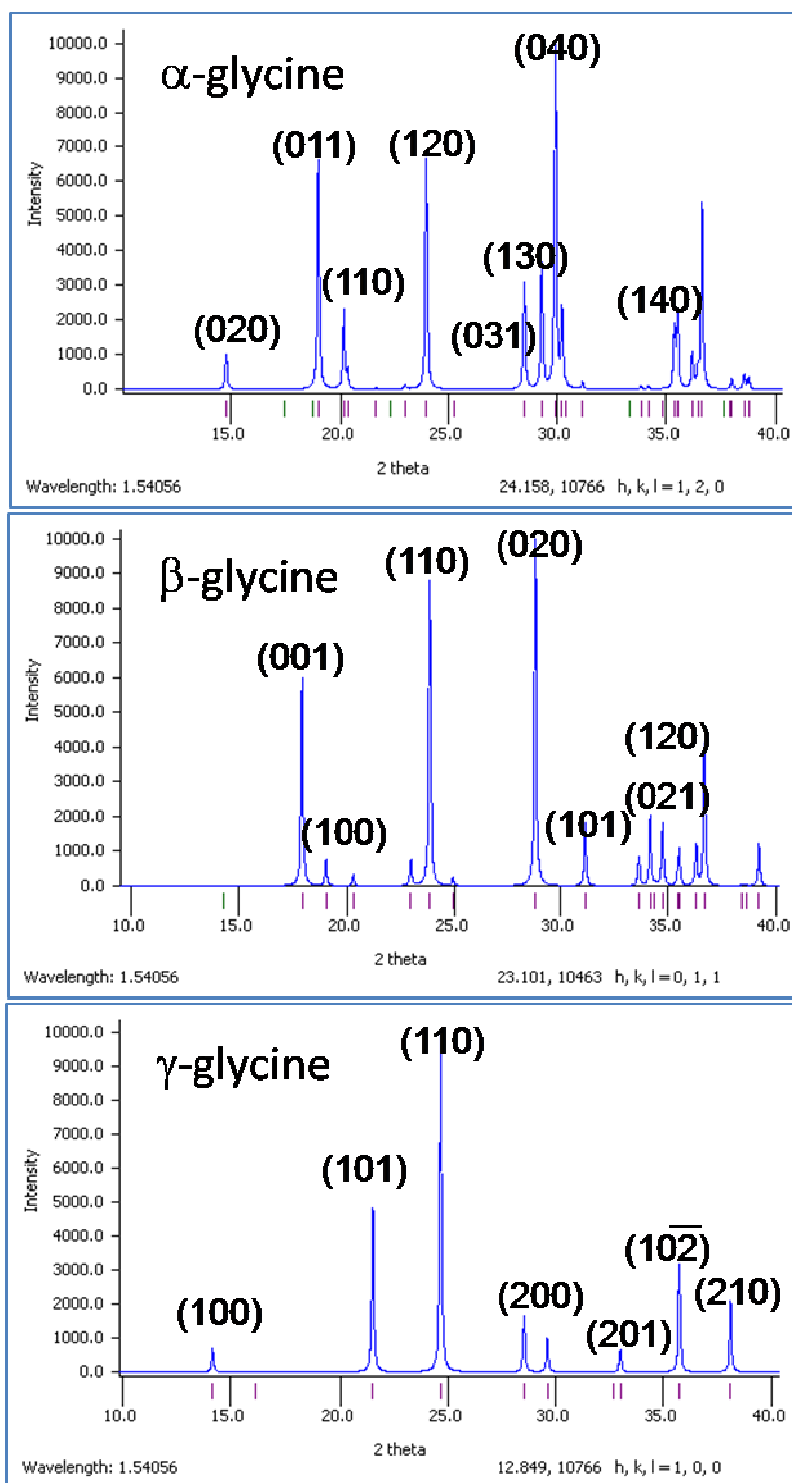
Figure S13. Simulated Powder X-Ray Diffraction patterns for α,-β- and γ-glycine crystals. The Miller indices correspoding to the peaks are also shown.
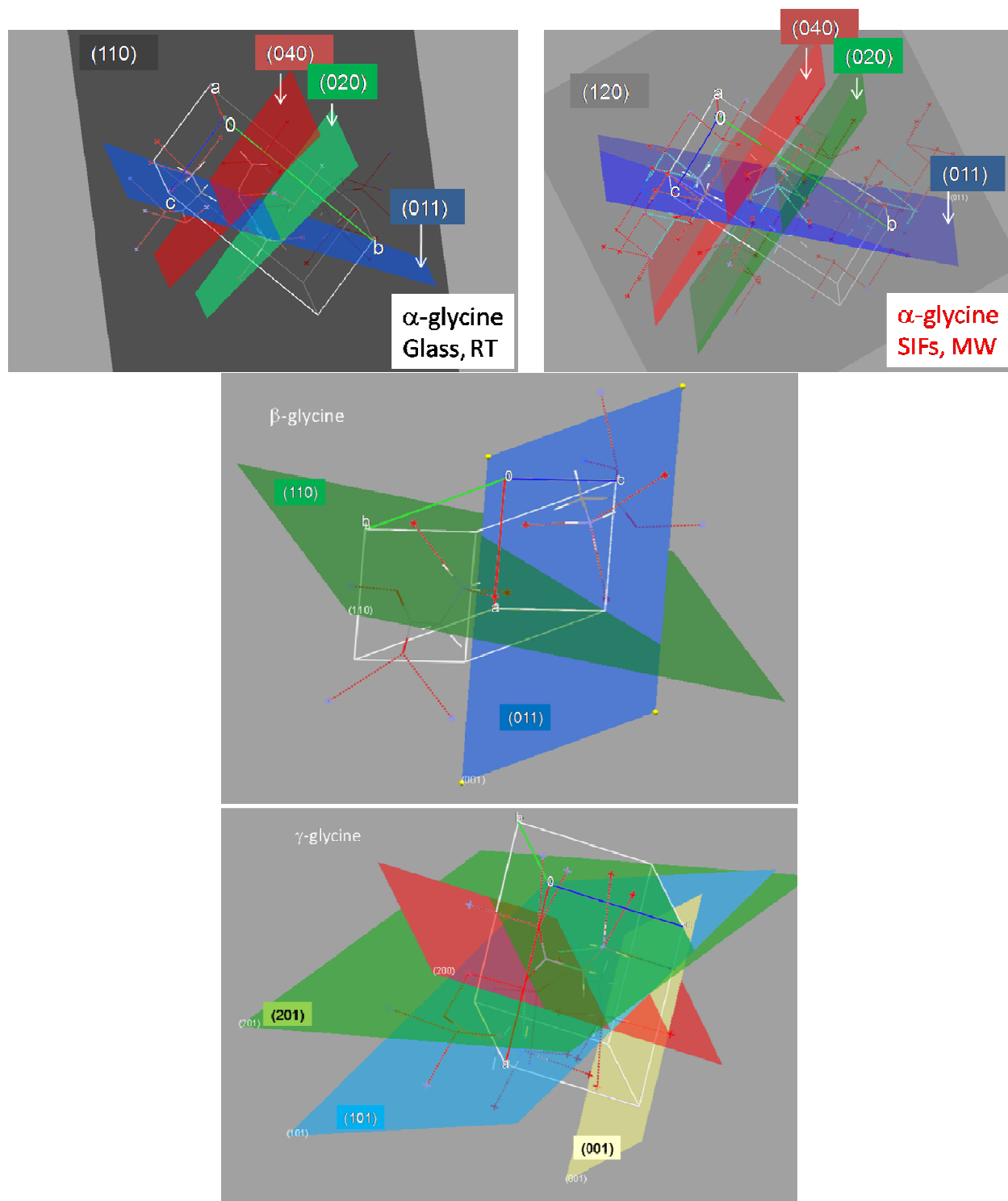
Figure S14. Simulated growth morphology of α–, β- and γ- glycine crystals, showing the selected crystal faces, which were observed in the experimental data. Hydrogen bonds are indicated as dashed red lines.

Cited references:

(1)   Ferrari, E. S.; Davey, R. J.; Cross, W. I.; Gillon, A. L.; Towler, C. S. *Crystal Growth & Design* **2003**, *3*, 53-60.

(2)   Dawson, A.; Allan, D. R.; Belmonte, S. A.; Clark, S. J.; David, W. I. F.; McGregor, P. A.; Parsons, S.; Pulham, C. R.; Sawyer, L. *Crystal Growth & Design* **2005**, *5*, 1415-1427.

(3)   Aslan, K.; Geddes, C. D. *Analyst* **2008**, *133*, 1469-80.

(4)   Hamilton, B. D.; Hillmyer, M. A.; Ward, M. D. *Crystal Growth & Design* **2008**, *8*, 3368-3375.

(5)   Hamilton, B. D.; Weissbuch, I.; Lahav, M.; Hillmyer, M. A.; Ward, M. D. *Journal of the American Chemical Society* **2009**, *131*, 2588-2596.

(6)   Lee, A. Y.; Lee, I. S.; Dettet, S. S.; Boerner, J.; Myerson, A. S. *Journal of the American Chemical Society* **2005**, *127*, 14982-14983.